Supplementary Information for

Evaluation of Drug Release from Polymeric Nanoparticles in Simulated Saliva and Gastric Media by Asymmetric Flow Field–Flow Fractionation (AF4)

Haoran Wu[1], Alaia Homawoo[2], Saba Shariati[3], Carlos E. Astete[4], Debora F. Rodrigues[1], Cristina M. Sabliov[4], Elham H. Fini[3], and Stacey M. Louie[1]*

[1]Department of Civil & Environmental Engineering, University of Houston, Houston, TX 77004

[2]Department of Electrical & Computer Engineering, University of Houston, Houston, TX 77004

[3]School of Sustainable Engineering and the Built Environment, Arizona State University, Tempe, AZ 85287, United States

[4]Department of Biological & Agricultural Engineering, Louisiana State University, Baton Rouge, LA 70803

[*] Corresponding Author:

Email: slouie@uh.edu

Phone: (713)-743-8646

Submitted to *RSC Pharmaceutics*

Pages: 19; **Figures:** 5; **Tables:** 4

S1. Literature Review

Table S1 provides an overview of the applications of asymmetric flow field–flow fractionation (AF4) for nanocarrier analysis.

Table S1. Summary of nanocarrier studies using AF4

Sample (Drug in Polymeric Carrier)	AF4 Method		Experimental Design		Reference
	Nanocarrier Characterization	Nanocarrier-associated Drug Detection	Sample Media	Release Study	
mRNA in DOTMA and DOPE liposome	SAXS: LPX structure; DLS: LPX R_h; MALS: LPX R_g, MW	UV: mRNA quantification; DLS: mRNA R_h; MALS: mRNA R_g, MW	Aqueous media	N/A	1
Quercetin-loaded nano-liposome	UV: liposome concentration; MALS: R_g, shape factor; DLS: R_h	N/A	Milli-Q water	N/A	2
Mitotane liposomes (DOPC-MT) and albumin-stabilized MT nanoparticles (BSA-MT)	UV: MT concentration; MALS: BSA-MT R_g	Off-line HPLC-DAD: DOPC-MT and BSA-MT	Purified water	N/A	3
Pb-DTPA in DSPC/cholesterol/DSPE-DTPA liposomes	UV/RI: Liposome concentration; MALS: Liposome R_g	γ-ray: quantification of Pb and radioactive decay products from the liposomes, and the size	Aqueous media with NaCl, HEPES and DTPA (pH 7.4)	N/A	4 *
Amphotericin B in liposomes	AF4-UV: Separation	Offine HPLC-UV-CAD: quantification of Amphotericin B, Cholesterol, DSPG and HSPC	Diluted with 5% dextrose solution	N/A	5 *
Doxorubicin in liposome	AF4: Separation Offline NTA/DLS: R_h	Offline LC-MS: Doxorubicin concentration	N/A (commercial products)	N/A	6 *
p-THPP in liposomes	UV: liposome concentration; MALS: liposome R_g	Offline HPLC–UV: p-THPP concentration	TRIS buffer	N/A	7 *

Sample (Drug in Polymeric Carrier)	AF4 Method		Experimental Design		Reference
	Nanocarrier Characterization	Nanocarrier-associated Drug Detection	Sample Media	Release Study	
Temoporfin and cholesterol in liposomes	MALS: liposome R_g	N/A	Glucose solution 5% (w/w)	N/A	8*
p-THPP in liposomes	UV: liposome concentration; MALS: liposome R_g	UV: p-THPP concentration	10 mM TRIS buffer (pH 7.4)	N/A	9
Sudan II, Sudan III, Sudan IV, Sudan V, Oil Red O, Sudan Black, p-THPP in liposomes	UV: liposome concentration; MALS: R_g	UV: drug concentrations	10 mM TRIS buffer (pH 7.4)	N/A	10
Egg phosphatidylcholine (egg-PC) in liposomes	UV/RI: liposome concentration; MALS: R_g	N/A	Aqueous medium	N/A	11
Aluminum chloride phthalocyanine in PEG-P(LA-co-BGE) nanospheres (NS)	UV: NS concentrations; MALS: NS R_g	Offline HPLC-FLD: quantification of AlClPc	Ultrapure water	FBS media *(release not quantified using AF4)*	12 *
Rose Bengal, Rhodamine B, DiI, 3-(α-azidoacetyl)coumarin, Nile Red, and IR780 in Polymeric nanosphere (NS) and oily core nanocapsule (NC) suspensions	UV: NS and NC concentration; MALS: R_g	Fluorescence: each dye and polymeric conjugate concentration	DMEM cell culture medium with 10% fetal bovine serum (FBS)	DMEM cell culture medium with 10% FBS	13
Lumogen®-loaded triglyceride-filled albumin-based nanocapsules (NC)	UV: albumin concentration; MALS: nanocapsule R_g	Fluorescence: Dye Lumogen® concentration	Purified water	N/A	14
IR-780 Iodide in PEG-PLA nanocapsules (NC)	UV: NC concentration; DLS: NC R_h; MALS: NC R_g	FLD: IR-780 concentration	Ultrapure water	PBS with polysorbate 80 (pH 7.4, 1% v/v) *(release not quantified using AF4)*	15 *

Sample (Drug in Polymeric Carrier)	AF4 Method		Experimental Design		Reference
	Nanocarrier Characterization	Nanocarrier-associated Drug Detection	Sample Media	Release Study	
Aluminum chloride phthalocyanine in PLA, PLA-PEG, PLA-chitosan nanocapsules (NC)	UV: NC concentrations; DLS: NC R_h; MALS: NC R_g, shape factor	Offline HPLC-FLD: quantification of AlClPc (a fluorescent marker for the labeled NC and extracted from NC and biological samples	Milli-Q water	PBS (pH 7.4), 37 °C *(release not quantified using AF4)*	16 *
Docetaxel and doxorubicin in liposomes, and SN-38 and daunorubicin in micelles	UV: micelles and liposomes concentrations; DLS: micelles and liposomes R_h; MALS: R_g	Offline HPLC-UV: Docetaxel, doxorubicin, SN-38, daunorubicin concentration	PBS	N/A	17 *
CRISPR-Cas9 ribonucleoprotein (RNP) in lipid nanoparticles (LNP)	DLS: LNP R_h	N/A	PBS with 25 mM imidazole	N/A	18
Oligonucleotide loaded Gelatin Nanoparticles (NP)	UV: NP concentration; MALS: R_g, Mw	UV: Oligonucleotide concentration	Milli-Q water	N/A	19
Single-stranded calf thymus DNA in chitosans (NAS-032 and NAS-075)	MALS: chitosan–DNA polyplex formation with different N/P ratios, MW, R_g, shape; DLS: R_h; UV/RI: concentration	N/A	Milli-Q water	N/A	20
Myoglobin (Mb) in PEG-b-(PDEAEMA-co-PDMAEMA-co-PDMIBMA polymersomes (Psome)	MALS: Psome M_w, M_n, R_g, shape factor; DLS: R_h; UV/RI: Mb-polymersomes concentration	UV/RI: Mb concentration	10 mM NaCl	N/A	21
Rose bengal-loaded (RB) polymersome (Psome)	MALS: RB-Psome R_g, shape factor; DLS: R_h	UV: RB concentration	10 mM PBS	10 mM PBS (pH 5 vs. 7.4) *(release not quantified using AF4)*	22

Sample (Drug in Polymeric Carrier)	AF4 Method		Experimental Design		Reference
	Nanocarrier Characterization	Nanocarrier-associated Drug Detection	Sample Media	Release Study	
Clofazimine (CLZ) in SBE-β-CD oligomers	RI: Oligomers concentration; MALS: R_g, molar mass	UV: CLZ concentration	Aqueous media	N/A	23 *
Curcumin in PMOXA-PDMS-PMOXA polymersomes (Psome)	UV: Psome concentrations; DLS: R_h; MLAS: R_g	FLD: Curcumin concentration	10 mM PBS (pH 7.4)	10 mM PBS with Tween 80 media (1%,v/v) *(release not quantified using AF4)*	24 *
Pheophorbide in PEO-b-PCL polymers	UV/RI: polymer concentration; QELS: polymer R_h; MALS: polymer R_g	UV: Pheophorbide concentration	Ultrapure water	N/A	25 *
Rose Bengal (RB) in polymer	UV: polymer concentration; MALS: polymer MW	UV: RB concentration	Pure water	N/A	26 *

*Note: Asterisks indicate articles before 2021 already summarized in the review article by Quattrini et al., [27].

Abbreviations: mRNA: messenger RNA; DOTMA: (R)-N,N,N-trimethyl-2-3-dioleyloxy-1-propanaminium chloride; DOPE: 1,2-dioleoyl-sn-glycero-3-phosphoethanolamine; N/A: not available; SAXS: small angle X-ray scattering; LPX: lipoplex; DLS: Dynamic light scattering; R_h: hydrodynamic radius; MALS: multi angle light scattering; R_g: radius of gyration; Mw: molecular weight; UV: UV-Vis spectroscopy; RI: refractive index; N/P: $[-NH_3^+]/[-PO_4^-]$ molar charge ratios; Shape factor: ($\rho = R_g/R_h$); Mb: Myoglobin; PEG-b-(PDEAEMA-co-PDMAEMA-co-PDMIBMA: poly(ethylene glycol)-b-(poly(diethylaminoethyl methacrylate)-co-poly(dimethylmaleimidobutyl methacrylate)); RB: Rose Bengal; Polymersome: Psome; PBS: Phosphate Buffered Saline; MT: Mitotane; DOPC: 1,2-dioleoyl-sn-glycero-3-phosphocholine; BSA: Bovine serum albumin; CRISPR-Cas9: clustered regularly interspaced short palindromic repeats (CRISPR) associated (Cas); RNP: ribonucleoprotein; LNP: lipid nanoparticle; DiI: 1,1′-dioctadecyl-3,3,3′,3′-tetramethyl-indocarbocyanine perchlorate; IR780: 2-[2-[2-chloro-3-[(1,3-dihydro-3,3-dimethyl-1-propyl-2H-indol-2-ylidene)ethylidene]-1-cyclohexen-1-yl]ethenyl]-3,3-dimethyl-1-propylindolium iodide: Nanosphere: NS; nanocapsule: NC; Dulbecco's Modified Eagle Medium: DMEM; FBS: Fetal bovine serum; DSPC: Diethylenetriamine-N,N,N′,N″,N″-pentaacetic acid; DSPC: 1,2-Distearoyl-sn-glycero-3-phosphorylcholine; DSPE: 1,2-Distearoyl-sn-glycero-3-phosphoethanolamine; HEPES: 2-[4-(2-hydroxyethyl)piperazin-1-yl]ethanesulfonic acid; PLA: poly(D,L-lactide); PLA-PEG: polyethylene glycol-block-poly(D,L-lactide); PLA-Cs: PLA with chitosan; AlClPc: [chloro(29H,31H-phthalocyaninato)aluminium; DSPG: 1,2-Distearoyl-sn-3-phosphoglycerol; HSPC: hydrogenated soy L-alpha-phosphatidylcholine; CLZ: Clofazimine; NTA: Nanoparticle tracking analysis; QELS: quasi-elastic light scattering; TRIS: (Tris(hydroxymethyl) aminomethane; RB: Rose Bengal; p-THPP: porphyrin 5,10,15,20-tetrakis(4-hydroxyphenyl)21H,23H-porphine; Egg-PC: Egg-phosphatidylcholine.

S2. PLGA-Enro NP Synthesis

An organic solution was prepared with 420 mg of PLGA and 39 mg of enrofloxacin, which were dissolved in 10 mL of ethyl acetate by stirring for 30 min at 400 to 500 rpm. An aqueous surfactant solution was prepared by dissolving 550 mg of Tween 80 in 110 mL of low resistivity water. An emulsion was prepared by adding the organic phase to the aqueous phase with stirring (400 to 500 rpm). The sample was then processed in a microfluidizer (M 110P, Microfluidics, Westwood, MA, USA) with four passes. The organic solvent was removed by rotary evaporation (Buchi R-300, Buchi Corp., New Castle, DE, USA) under vacuum at 32 ° C for 70 min. An aqueous PVA solution was prepared using 180 mg PVA in 9 mL of water and added to the NP suspension. Finally, 1189 mg of trehalose was added as a cryoprotectant, and the NPs were freeze-dried (FreeZone 2.5, Labconco Corp., Kansas City, MO, USA) at –80 ° C for 2 d. The NPs were stored at –20 °C until use.

S3. Release Media Preparation

The media used for the release experiments are reported in Table S2. Chemicals used for media preparation included NaCl (ACS grade, VWR Chemicals, Solon, OH, USA), KCl (ACS grade, EMD Millipore, Billerica, MA, USA), $Na_2HPO_4 \cdot 7H_2O$ (ACS grade, VWR Chemicals, Solon, OH, USA), KH_2PO_4 (ACS grade, Amresco, Solon, OH, USA), HCl (ACS grade, Sigma Aldrich, St. Louis, MO, USA), α-amylase (from porcine pancreas, Type VI-B, ≥ 5 units/mg solid, Sigma Aldrich, St. Louis, MO, USA), and pepsin (from porcine gastric mucosa, ≥ 250 units/mg solid, Sigma Aldrich, St. Louis, MO, USA).

Table S2. Composition and properties of release media

Media	Composition	Ionic Strength	pH
PBS	137 mM NaCl 2.7 mM KCl 10.1 mM Na_2HPO_4 1.8 mM KH_2PO_4	211.1 mM	7.4 ± 0.1
Simulated saliva	2 g/L (34 mM) NaCl 0.5 g/L α-amylase*	34 mM	6.8 ± 0.1
SGF	10 mM HCl 2 g/L (34 mM) NaCl 3.2 g/L pepsin	44 mM	2.5 ± 0.1

*The simulated saliva and SGF were prepared and tested with or without the protein

S4. Batch Total Organic Carbon (TOC) Analysis for Protein Loss in Filtration

Simulated saliva containing amylase and SGF containing pepsin were filtered prior to use. The protein concentrations in the unfiltered and filtered samples were compared by batch TOC analysis using the grab method measurement mode (Sievers M9 SEC, Suez Water Technologies, Trevose, PA, USA). The samples were diluted in deionized water by a dilution factor of 160 prior to analysis. The TOC analyzer was set to draw sample continuously at 0.5 mL/min, with a 10 min initial flush time followed by five replicate measurements of 2 min duration. Phosphoric acid (6 M) was injected at 2.0 μL/min for inorganic carbon removal, and a buffered ammonium persulfate solution (150 g/L in phosphate buffer) was injected at 13.0 μL/min to oxidize organic carbon to CO_2 for detection. The signals for the last 3 measurement replicates were averaged per sample, with triplicate samples prepared and analyzed for each unfiltered and filtered protein solution.

S5. Drug Release at 37 °C

Figure S1 compares the drug release at 37 °C in the various media. The same trend was observed across all five media as in the experiments at 30 °C, but the rapid rate of release and nearly-complete release in the SGF media by 2 hours introduces uncertainty in the release time points, as some time is required to collect sample out of the heated bath and perform the AF4 analyses. Hence, all other experiments were conducted at 30 °C, where slower release is achieved and there is lower relative uncertainty in the sampling time points.

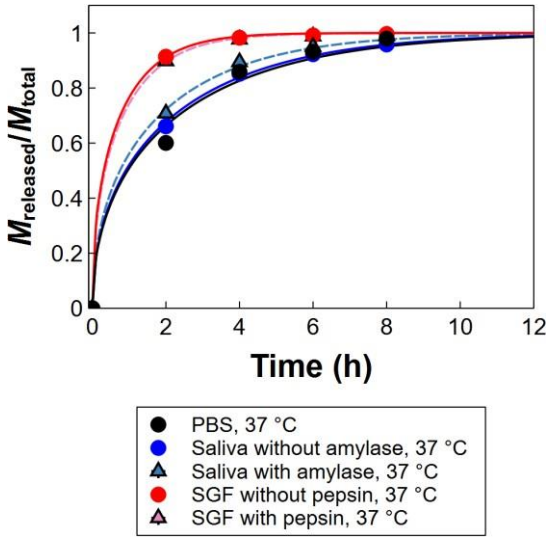

Figure S1. Drug release profiles and radial diffusion model fits for PLGA-Enro NPs in various release media at 37 °C for up to 8 hours. Preliminary data were collected on single experiments.

S6. AF4 Method Details

The AF4 method for the PLGA-Enro NPs was applied using the settings optimized in our prior method development study.[28] Table S3 presents the AF4 separation method, i.e., focus flow and crossflow settings and durations. The detector flow rate was 0.5 mL/min throughout the entire measurement run. During the sample injection steps, the injection flow rate was 0.2 mL/min.

Table S3. Crossflow rates and duration of each separation step in the AF4 method

Mode	Duration (min)	Crossflow rate (mL/min)
Elution	6	0.15
Focus	1	1.5
Focus + Injection	4	1.5
Elution	58	0.15
Elution + Injection	15	0
Elution	6	0
Elution	10	0.15

The online detectors connected to the AF4 effluent were ordered as (1) UV diode array detector (DAD), (2) multi-angle light scattering (MALS) / dynamic light scattering (DLS) detector, (3) fluorescence detector (FLD), (4) differential refractive index (dRI) detector, and (5) total organic carbon (TOC) detector, following the pressure limits (high to low) of each detector and the destructive nature of the TOC analysis. Bovine serum albumin (BSA) was run as a calibration standard in a buffer comprised of 4 mM phosphate and 25 mM NaCl (pH ≈ 7) with the same detector flow (0.5 mL/min) and a higher crossflow during the focus and elution stages (2.0 mL/min). The BSA was used for detector alignment, band broadening correction, and MALS detector normalization.

S7. Additional Release Models

Two additional release models were applied to the drug release data for comparison against the radial diffusion model:

(a) First-order kinetic model:

$$\frac{M_{\text{released}}}{M_{\text{total}}} = 1 - \exp(-k_{\text{first order}} t) \quad \text{(S1)}$$

This model predicts the fraction of drug mass released ($M_{\text{released}}/M_{\text{total}}$) over time (t) to follow first order kinetics with rate constant $k_{\text{first order}}$. The model assumes perfect sink conditions and homogeneous drug distribution in the particles at all times. These assumptions are not expected to be representative of the PLGA-Enro nanoparticles, but the model is evaluated for comparison since it is frequently applied to drug release profiles.

(b) Erosion model:[29]

$$\frac{M_{\text{released}}}{M_{\text{total}}} = 1 - (1 - k_{\text{erosion}} t)^3 \quad \text{(S2)}$$

This model assumes that the drug is homogeneously distributed within the polymer matrix and only releases upon erosion of the particle, i.e., it does not dissolve or diffuse out of the particles. The polymer mass erosion rate (i.e., rate of decrease in the particle volume) is assumed to be proportional to the outer surface area of the spherical particles. The rate constant k_{erosion} represents a lumped constant comprising the erosion rate (nm/s) along with geometric factors (relating surface area and volume) and mathematical integration factors. The model was fitted to only the first 90% of drug release, as the cubic model equation above is not limited to a maximum release of 100%.

S8. Zeta Potential Results

The measured zeta potentials of the PLGA-Enro NPs in the various media at the beginning (0 h) and end (48 h) of the release experiments are provided in Figure S2.

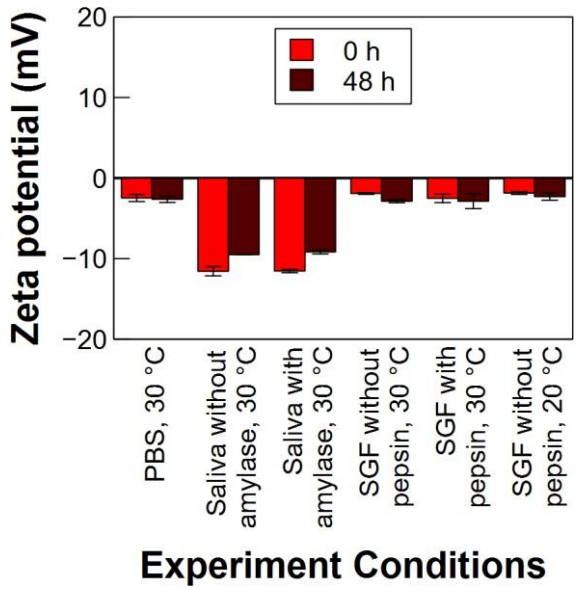

Figure S2. Measured zeta potentials of the PLGA-Enro NPs between 0 and 48 h in all release experiment conditions tested. Samples were diluted from 15 g/L to 1 g/L of PLGA-Enro NPs (as total lyophilized powder), resulting in an ionic strength and pH of 14.1 mM (pH 7.2) for PBS, 2.3 mM (pH 5.6 to 6.0) for saliva with or without amylase, and 2.9 mM (pH 3.4 to 3.6) for SGF with or without pepsin. Error bars represent standard deviations on triplicated experiments.

S9. AF4-TOC Results

The online TOC detector could be used to quantify the PLGA-Enro NPs. Figure S3 shows an example of the AF4-TOC chromatograms and fluorescent drug release analysis using the TOC signal for NP quantification for PLGA-Enro NPs in SGF without pepsin at 30 °C. Because the samples contained excess polyvinyl alcohol surfactant in the NP formulation (and biomolecules in the media containing proteins), a large void peak corresponding to these species appears in the AF4-TOC chromatograms, complicating the analysis of the NP peak by TOC detection.

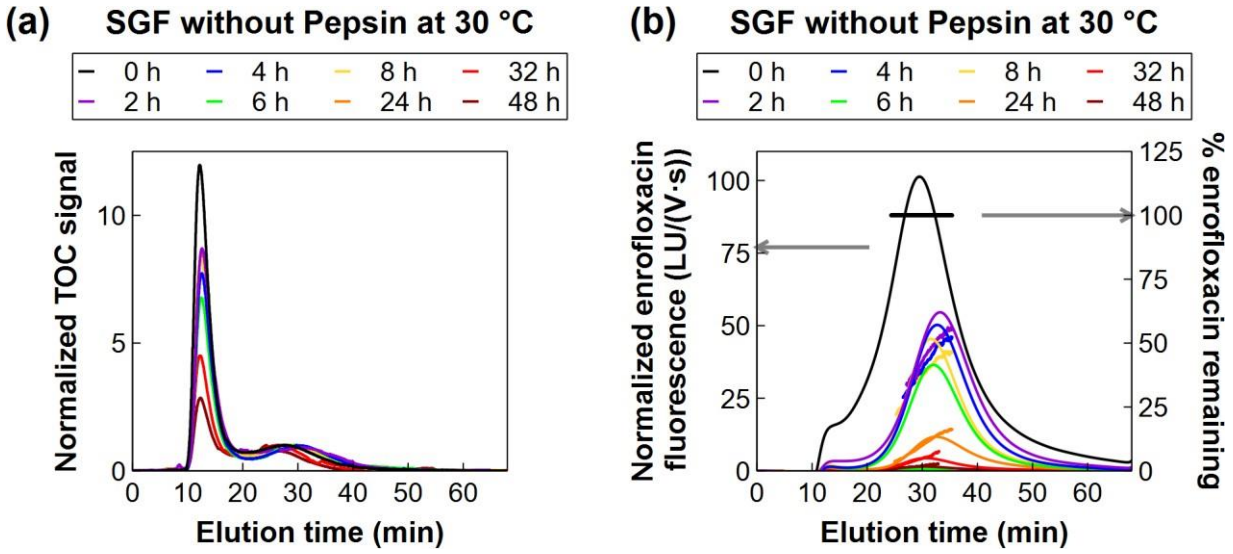

Figure S3. AF4-TOC chromatograms for quantifying PLGA NPs (a), AF4-FLD chromatograms for quantifying enrofloxacin loading (left axis of b), and percentages of enrofloxacin remaining at each elution time point (right axis of b). The data were processed as in Figure 2, except using the TOC signal in place of the UV signal. Representative chromatograms are shown for one experiment of a total of three replicates per release media.

S10. AF4-UV-FLD Results for Enrofloxacin Release in Media with Proteins or at 20 °C

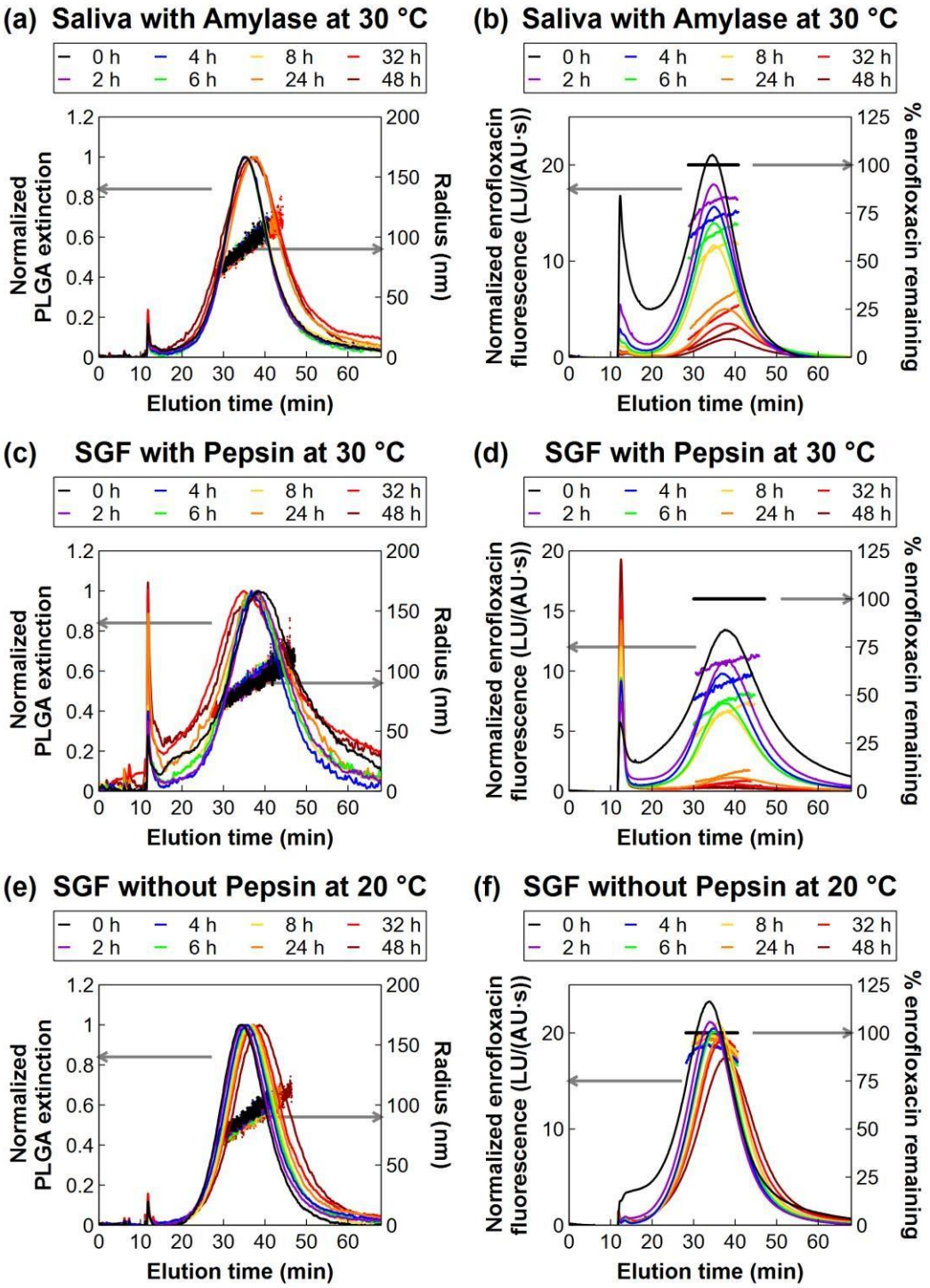

Figure S4. AF4-UV chromatograms and online DLS measurements (a, c, and e), AF4-FLD analyses (b, d, and f) for enrofloxacin release in media with proteins or at 20 °C. Representative chromatograms are shown for one experiment of a total of three replicates per release media.

S11. Model Fitting on the Bulk Drug Release Profiles

Table S4 provides the best-fit radial diffusion rate constant and diffusion coefficient determined for the PLGA-Enro NPs in each release medium, along with the 95% confidence intervals on the model fits.

Table S4. Radial Diffusion Model Fitting Parameters for Release in Various Conditions

Experiment Condition	Fitted Parameters[†]	
	$k_{\text{radial diffusion}}$ (h^{-1})	D ($cm^2\ s^{-1}$)
PBS, 30 ℃	0.0017 (0.0013, 0.0021)	5.0×10^{-17} $(3.9, 6.2) \times 10^{-17}$
Saliva without amylase, 30 ℃	0.0024 (0.0021, 0.0029)	5.9×10^{-17} $(5.0, 6.9) \times 10^{-17}$
SGF without pepsin, 30 ℃	0.0098 (0.0087, 0.0109)	22×10^{-17} $(20, 24) \times 10^{-17}$
Saliva with amylase, 30 ℃	0.0040 (0.0036, 0.0044)	9.3×10^{-17} $(8.4, 10.3) \times 10^{-17}$
SGF with pepsin, 30 ℃	0.0073 (0.0064, 0.0083)	16×10^{-17} $(14, 18) \times 10^{-17}$
SGF without pepsin, 20 ℃	0.00005 (0.00001, 0.00012)	0.13×10^{-17} $(0.03, 0.30) \times 10^{-17}$

[†]Fitted parameters are presented as the best-fit value on the triplicated release experiments, followed by the upper and lower bounds of the 95% confidence interval on the model fit in parentheses.

S12. Evaluation of Drug-Protein Interactions in Solution

Proteins elute in the void peak during the AF4 measurements of the PLGA-Enro NPs. Hence, drug-protein interactions could be probed by evaluating the enrofloxacin fluorescence signal in the void peak (Figure S5). In control injections of the protein-containing media (without NPs), amylase did not contribute any fluorescence at the excitation/emission wavelengths used for enrofloxacin detection, whereas pepsin did. In all media, the void peak fluorescence was initially high (likely from free enrofloxacin initially present in the NP formulation), but decreased to the background fluorescence signal for the proteins alone over the course of the release experiment. In addition, the rate of free enrofloxacin depletion was similar for protein-containing and protein-free media. These results suggest that there were no significant drug-protein interactions.

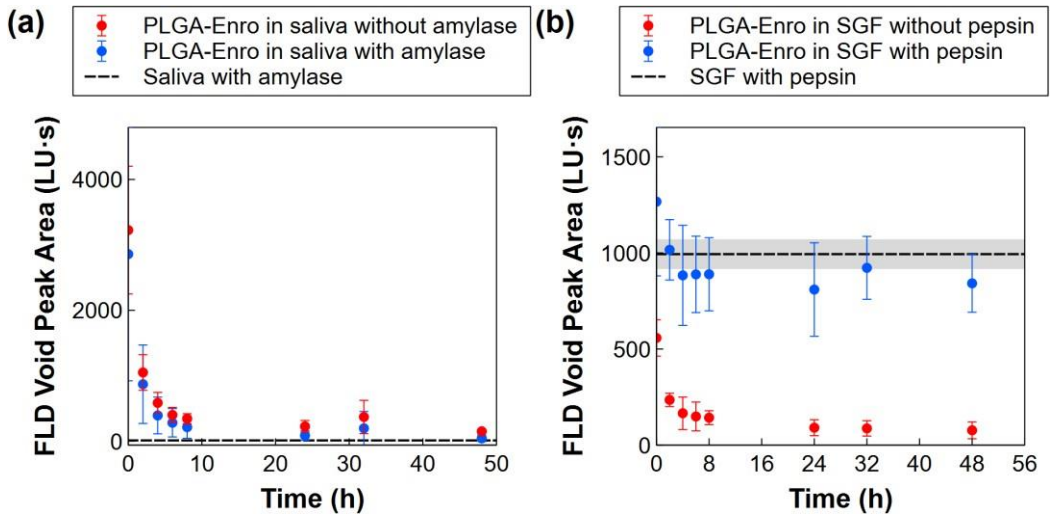

Figure S5. Fluorescence void peak areas for the PLGA-Enro NPs in saliva with or without amylase (a) and SGF with or without pepsin (b) at 30 °C, along with fluorescence peak area for control measurements on the proteins in the media (without NPs). Error bars represent standard deviations on triplicate release experiments, and shaded bounds represent standard deviations on triplicate measurements of the pepsin in SGF.

References

1. M. A. Graewert, C. Wilhelmy, T. Bacic, J. Schumacher, C. Blanchet, F. Meier, R. Drexel, R. Welz, B. Kolb, K. Bartels, T. Nawroth, T. Klein, D. Svergun, P. Langguth and H. Haas, *Sci. Rep.*, 2023, **13**, 15764.
2. S. Melchior, M. Codrich, A. Gorassini, D. Mehn, J. Ponti, G. Verardo, G. Tell, L. Calzolai and S. Calligaris, *Food Chem.*, 2023, **428**, 136680.
3. C. Langer, M. Köll-Weber, M. Holzer, C. Hantel and R. Süss, *Pharmaceutics*, 2022, **14**, 1891.
4. S. Huclier-Markai, A. Grivaud-Le Du, E. N'tsiba, G. Montavon, M. Mougin-Degraef and J. Barbet, *J. Chromatogr. A*, 2018, **1573**, 107-114.
5. D. Van Haute, W. Jiang and T. Mudalige, *Int. J. Pharm.*, 2019, **569**, 118603.
6. S. M. Ansar and T. Mudalige, *Int. J. Pharm.*, 2020, **574**, 118906.
7. A. H. Hinna, S. Hupfeld, J. Kuntsche and M. Brandl, *J. Pharm. Biomed. Anal.*, 2016, **124**, 157-163.
8. C. Decker, A. Fahr, J. Kuntsche and S. May, *Chem. Phys. Lipids*, 2012, **165**, 520-529.
9. A. Hinna, F. Steiniger, S. Hupfeld, M. Brandl and J. Kuntsche, *Anal. Bioanal. Chem.*, 2014, **406**, 7827-7839.
10. A. H. Hinna, S. Hupfeld, J. Kuntsche, A. Bauer-Brandl and M. Brandl, *J. Controlled Release*, 2016, **232**, 228-237.
11. S. Hupfeld, D. Ausbacher and M. Brandl, *J. Sep. Sci.*, 2009, **32**, 3555-3561.
12. G. E. N. Pound-Lana, G. M. Garcia, I. C. Trindade, P. Capelari-Oliveira, T. G. Pontifice, J. M. C. Vilela, M. S. Andrade, B. Nottelet, B. B. Postacchini and V. C. F. Mosqueira, *Mater. Sci. Eng., C*, 2019, **94**, 220-233.

13. M. A. de Oliveira, G. Pound-Lana, P. Capelari-Oliveira, T. G. Pontífice, S. E. D. Silva, M. G. C. Machado, B. B. Postacchini and V. C. F. Mosqueira, *J. Chromatogr. A*, 2021, **1641**, 461959.

14. S. Hester, K. B. Ferenz, A. Adick, C. Kakalias, D. Mulac, S. Azhdari and K. Langer, *Int. J. Pharm.*, 2023, **646**, 123454.

15. M. G. C. Machado, G. Pound-Lana, M. A. de Oliveira, E. G. Lanna, M. C. P. Fialho, A. C. F. de Brito, A. P. M. Barboza, R. D. d. O. Aguiar-Soares and V. C. F. Mosqueira, *Drug Delivery Transl. Res.*, 2020, **10**, 1626-1643.

16. L. T. Oliveira, M. A. de Paula, B. M. Roatt, G. M. Garcia, L. S. B. Silva, A. B. Reis, C. S. de Paula, J. M. C. Vilela, M. S. Andrade, G. Pound-Lana and V. C. F. Mosqueira, *Eur. J. Pharm. Sci.*, 2017, **105**, 19-32.

17. Y. Hu, R. M. Crist and J. D. Clogston, *Anal. Bioanal. Chem.*, 2020, **412**, 425-438.

18. J. Walther, D. Wilbie, V. S. J. Tissingh, M. Öktem, H. van der Veen, B. Lou and E. Mastrobattista, *Pharmaceutics*, 2022, **14**, 213.

19. W. Fraunhofer, G. Winter and C. Coester, *Anal. Chem.*, 2004, **76**, 1909-1920.

20. A. Sajid, M. Castronovo and F. M. Goycoolea, *Polymers*, 2023, **15**, 2115.

21. M. Palinske, U. L. Muza, S. Moreno, D. Appelhans, S. Boye, R. Schweins and A. Lederer, *Macromol. Chem. Phys.*, 2023, **224**, 2200300.

22. K. Sztandera, M. Gorzkiewicz, X. Wang, S. Boye, D. Appelhans and B. Klajnert-Maculewicz, *Colloids Surf., B*, 2022, **217**, 112662.

23. J. Wankar, F. Bonvicini, G. Benkovics, V. Marassi, M. Malanga, E. Fenyvesi, G. A. Gentilomi, P. Reschiglian, B. Roda and I. Manet, *Mol. Pharmaceutics*, 2018, **15**, 3823-3836.

24. A. Moquin, J. Ji, K. Neibert, F. M. Winnik and D. Maysinger, *ACS Omega*, 2018, **3**, 13882-13893.

25. J. Ehrhart, A.-F. Mingotaud and F. Violleau, *J. Chromatogr. A*, 2011, **1218**, 4249-4256.

26. S. Boye, N. Polikarpov, D. Appelhans and A. Lederer, *J. Chromatogr. A*, 2010, **1217**, 4841-4849.

27. F. Quattrini, G. Berrecoso, J. Crecente-Campo and M. J. Alonso, *Drug Delivery Transl. Res.*, 2021, **11**, 373-395.

28. S. Shakiba, C. E. Astete, R. Cueto, D. F. Rodrigues, C. M. Sabliov and S. M. Louie, *J. Controlled Release*, 2021, **338**, 410-421.

29. J.-M. Vergnaud, *Controlled Drug Release of Oral Dosage Forms*, Ellis Horwood, New York, NY, 1993.